SAND2008-3097C

X-ray Diagnostics of Imploding Plasmas from Planar Wire Arrays Composed of Cu and Few Tracer Al Wires on the 1MA Pulsed Power Generator at UNR

A. S. Safronova, V.L. Kantsyrev, A. A. Esaulov, N. Ouart, M. F. Yilmaz, K. Williamson, V. Shlyaptseva, I. Shrestha, G. Osborne,
University of Nevada, Reno, NV

C. A. Coverdale, B. Jones *Sandia National Laboratories, Albuquerque, NM*

C. Deeney, *NNSA, DOE, Headquarters, Washington DC*

17th Topical Conference High-Temperature Plasma Diagnostics

(Albuquerque, NM, May 11-15, 2008)

Sandia National Laboratories

ABSTRACT

Aluminum alloyed wires (Al5056) were traditionally used in x-ray diagnostics of implosions of cylindrical wire arrays produced on 6 MA Saturn and 20 MA Z generators at Sandia National Laboratories as well as on the university-scale 1 MA Z-pinch generators. We found another approach when 1-2 wires of the main material were replaced by Al wires (that constitute less than 20% of the total mass of the load) very useful in diagnostics of wire array plasmas from mid-z elements. Specifically, the analysis of combined planar wire array (PWA) experiments using the advanced set of x-ray diagnostics is presented. In these experiments, which were conducted at the 1 MA pulsed power generator at UNR, the Z-pinch load consisted of several (8) Cu alloyed and 1-2 Al alloyed wires mounted in a single row (both for single and double PWA). Implosion and radiative characteristics of such PWAs were studied using filtered PCD and XRD detectors, a bare bolometer, time-gated and time-integrated pinhole cameras, and time-integrated, spatially resolved and time-gated spatially integrated spectrometers. Special emphasis is made on dependence of x-ray spectra on the percentage of Al (5-19%) in the total mass of the load. The comparison with the results of experiments with uniform PWAs from Al alloyed wires on the same Z-pinch generator is discussed. The advantage of using such tracer diagnostics in wire array experiments is highlighted.

INTRODUCTION

Aluminum alloyed wires (Al5056) were traditionally used in x-ray diagnostics of implosions of cylindrical wire arrays produced on 6 MA Saturn and 20 MA Z generators at Sandia National Laboratories as well as on the university-scale 1 MA Z-pinch generators. The K-shell Al plasmas produced in such implosions is usually optically thick and thus challenging for diagnostics. The diagnostic method of radiation from such wire array implosions was suggested, successfully applied, and described in many publications by J.P. Apruzese et al (see, for example, [1,2]). It is based on the use of the alloyed Al 5056 wires which have 95% Al and 5% Mg. K-shell Mg lines are much less influenced by opacity because of their relative low concentration and are very helpful in diagnostics of optically thick K-shell plasmas. We found another approach that replaced 1-2 wires of the main material with Al wires (that constitute less than 20% of the total mass of the load) to be very useful in diagnostics of wire array plasmas from mid-z elements. Specifically, the analysis of combined planar wire array (PWA) experiments using the advanced set of x-ray diagnostics is presented. In these experiments, which were conducted at the 1 MA pulsed power generator at UNR, the Z-pinch load consisted of several (8) Cu alloyed and 1-2 Al alloyed wires mounted in a single row (both for single and double PWA). The most intense K-shell Al lines and L-shell Cu lines from high-Rydberg states $n \geq 4$ occupy the same spectral region from 6.5 to 9.5 Å and are both generated by plasmas with similar electron temperatures close to 300 eV. This makes the use of Al tracer wires an additional and valuable diagnostic tool for mid-z element plasmas.

1. **J.P. Apruzese, J.W. Thornhill, K.G. Whitney *et al*, Phys. Plasmas 8, 3799 (2001)**
2. **J.P. Apruzese, J. Davis, K.G. Whitney *et al*, Phys. Plasmas 9, 2411 (2002)**

Planar wire arrays (SPWA and DPWA)

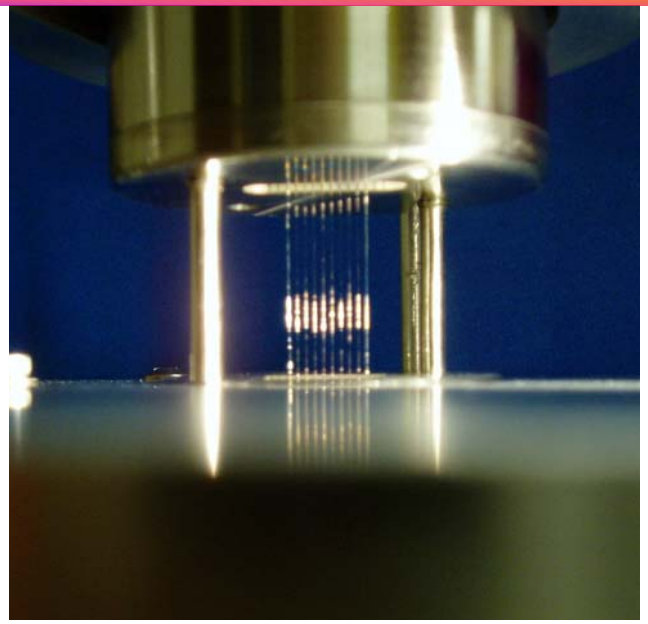

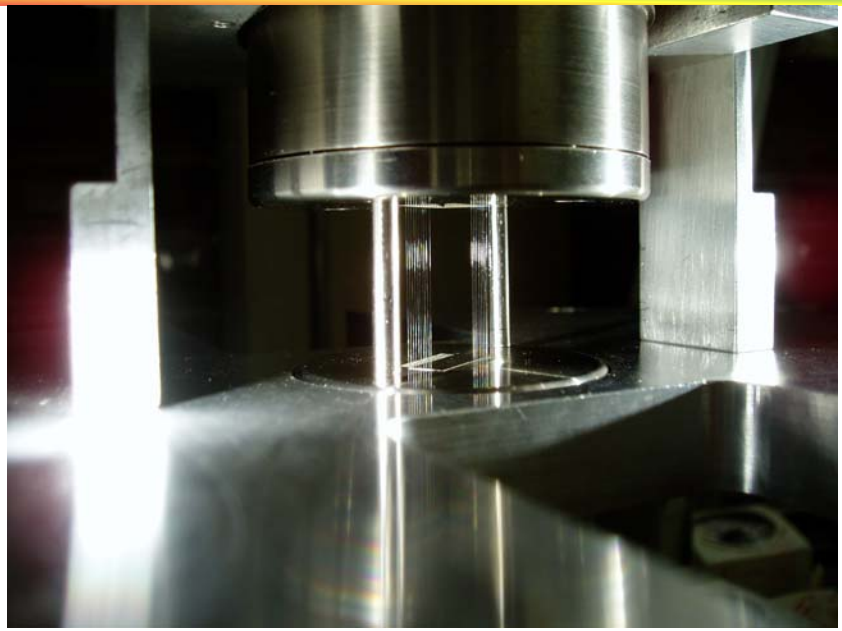

Single Planar Wire Array (SPWA)

Number of wires 10-15
Wire diameter 7-20 μm
Length of wire 20 mm
Gap between wires 0.7-1 mm

Double Planar Wire Array (DPWA)

Number of wires in each plane 8-15
Wire diameter 7-20 μm
Length of wire 20 mm
Gap between wires 0.7-1 mm
Gap between planes 1.5-9 mm

For more about the studies of implosion and radiative characteristics of planar wire arrays as well as for details of diagnostics see:

3. **V.L. Kantsyrev, L.I. Rudakov, A.S. Safronova *et al*, IEEE 34, 196 (2006)**
4. **V.L. Kantsyrev, L.I. Rudakov, A.S. Safronova *et al*, Phys. Plasmas 15, 030704 (2008)**

Table 1. Details of load types and configurations.

Shot N	Date	Load	N of wires	Mass (μg)	Al mass (%)	Bolo (kJ)	Load details
782	8/7/06	SPWA	10	143	18.5	14.4	
801	7/17/06	SPWA	15	143	100	10.4	
1293	10/25/07	DPWA	9x9	259	11.3	17.6	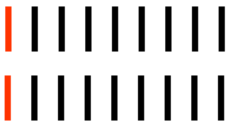

- Al wires shown in red have Φ=17.8 μm in Al5056/Cu loads and 15 μm in Al5052 load
- Cu wires (Ni 60, 96%Cu and 4% Ni) shown in black have Φ =10.16 μm

EXPERIMENTAL AND THEORETICAL DIAGNOSTIC TOOLS

Experiments were performed on 1 MA Zebra generator at University of Nevada, Reno (UNR). Wire array loads were planar wire arrays (PWA) in two different configurations: single planar (SPWA) and double planar (DPWA) wire arrays. SPWA had 10 wires arranged in a single plane with an interwire gap of 1 mm. DPWA had two planes located at the distance of 1.5 mm with 9 wires in each plane with an interwire gap of 0.7 mm. Both SPWA and DPWA consisted mainly from Cu wires (alloy Ni60, 96% Cu and 4% Ni) while 1 or 2 wires of the main Cu material were replaced by Al (alloy Al5056, 95% Al and 5% Mg) wires at the edge of the array. The details of the load configurations are listed in Table 1. Implosion and radiative characteristics of such PWAs were studied using filtered PCD and XRD detectors, a bare Ni bolometer, time-gated and time-integrated pinhole cameras, and time-integrated, spatially resolved and time-gated spatially integrated spectrometers (the details of experiments with SPWA and DPWA can be found in [3,4]). The typical suite of x-ray data collected in the PWA experiments relevant to this study is shown in next slides.

3. V.L. Kantsyrev, L.I. Rudakov, A.S. Safronova *et al*, IEEE 34, 196 (2006)
4. V.L. Kantsyrev, L.I. Rudakov, A.S. Safronova *et al*, Phys. Plasmas 15, 030704 (2008)

EXPERIMENTAL AND THEORETICAL DIAGNOSTIC TOOLS (continued)

Non-LTE collisional-radiative atomic kinetic model of Cu has been employed in this work [5, 6]. This model includes all the ground states from the bare ion to the neutral atom as well as atomic structure details for some of the ions. In particular, singly-excited states up to n=5 are taken into account with the exception of H-like and Be-like (which included up to n=6 and n=4, respectively). Doubly-excited states and a total number of levels in each model are specified below. The energy level structure and complete radiative and collisional coupling was calculated by the FAC code [7]. The Cu model includes the details of the ions from H-like to Al-like for a total of 3719 levels. This model was already successfully applied to study L- and K-shell radiation from X-pinches on 1 MA Zebra at UNR [5] as well as L-shell Cu radiation from nested wire arrays on 20 MA SNL-Z [6]. In addition, non-LTE atomic kinetic model of Al was applied to estimate plasma parameters for K-shell Al plasmas. The description of the model as well as its application to wire arrays experiments on 1 MA Z-pinch generators can be found in [8,9].

5. AS. Safronova, V. L. Kantsyrev, N. D. Ouart *et al*, JQSRT 99, 560 (2006)
6. C.A. Coverdale, B. Jones, P.D. LePell, A.S. Safronova, V.L.Kantsyrev, D.A. Fedin. N.D. Ouart *et al*, AIP Proceedings 808, 6th International Conference on Dense Z-Pinches, 45 (2006)
7. M.F. Gu, AIP Conference proceedings 730, 127 (2004)
8. D.J. Ampleford, S.V, Lebedev, S,N, Bland *et al*, Phys. Plasmas 14, 102704 (2007)
9. A.S. Safronova, V.L. Kantsyrev, A.A. Esaulov *et al*, Phys. Plasmas 15, 033302 (2008)

X-ray time-gated pinhole images and spectra and their analysis

Fig. 1 presents PCD (8 μm Be filter) detector (that registered x-ray radiation with hν > 0.75 keV) and current data as well as time-gated pinhole (TGPH) images taken along the PWA plane in two spectral region: hν >1 keV (top row) and hν >3 keV (bottom row) for DPWA (shot 1293). In addition, the location of MCP for TGPH images (labeled 1-6) as well as for time-gated spectra (TGSP) images (labeled 1'-5') is shown. Implosion of the DPWA (shot 1293) is characterized by the main x-ray burst almost at the peak of the current with subsequent less intense x-ray bursts (following about every next 10 nsec) as well as by the formation of hot spots (see Fig. 1). Hot spots are formed first near the anode (recorded by the 1^{st} frame at ~14 nsec and 2^{nd} frame at ~9 nsec before the main x-ray burst) then moved towards the cathode (recorded by the 5^{th} at ~ 12 nsec and 6^{th} at ~ 17 nsec after the main x-ray burst). The image of TGSP along with lineouts of spectra recorded by all 5 frames and 3^{rd} and 4^{th} frames and theoretical modeling is shown in Fig. 2. The spectra recorded by the KAP crystal cover the spectral region from 7 to 11 Å and include K-shell Al and L-shell Cu lines. The most intense K-shell Al lines are He- and H-like resonance lines: Heα at 7.758 Å labeled Al1 ($1s2p\ ^1P_1 - 1s^2\ ^1S_0$), Lyα at 7.171 Å labeled Al2 ($2p\ ^2P_{1./2,3/2} - 1s\ ^2S_{1/2}$), and Heβ at 6.635 Å labeled Al3 ($1s3p\ ^1P_1 - 1s^2\ ^1S_0$). The most intense L-shell Cu lines are Ne-like resonance lines due to 3-2 transitions 3A-3G that occupy the spectral region from 10.58 to 12.85 Å with the most intense lines 3C at 11.390 Å and 3D at 11.608 Å not shown here. It is convenient to use for diagnostics the less intense Ne-like lines from high Rydberg state n=4 and even higher n=5 and 6 (which are expected to be less effected by opacity than 3C and 3D lines) such as, for example, lines 4C at 9.115 Å ($1s^22s^22p^54d\ ^1P_1 - 1s^22s^22p^6\ ^1S_0$) and 4D at 9.245 Å ($1s^22s^22p^54d\ ^3D_1 - 1s^22s^22p^6\ ^1S_0$). Also, F-like Cu lines are important for diagnostics because they are observed at the temperatures higher than Ne-like Cu lines. One of these lines at 10.85 Å labeled F1 is shown in Fig. 2.

Fig. 1. Zebra shot 1293. PCD (8 μm Be filter) detector that registered x-ray radiation with hν > 0.75 keV (gray) and current (red) data. Note "hot spot"- like plasma formation for DPWA

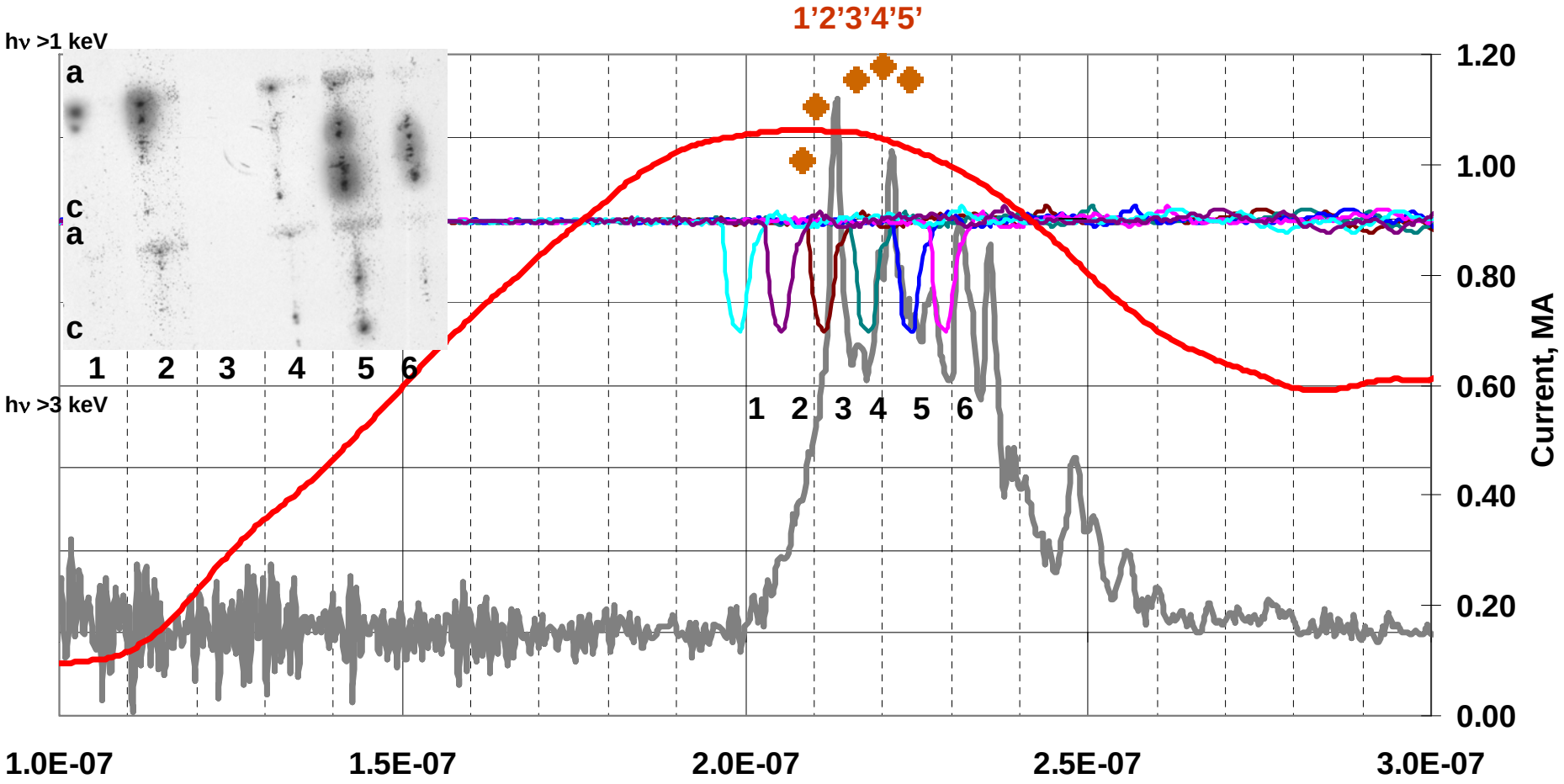

The time-gated pinhole (TGPH) images taken along the PWA plane in two spectral region: hν >1 keV (top row) and hν >3 keV (bottom row) in the left upper corner. At the top, the location of MCP for TGPH images (labeled 1-6) and for time-gated spectra (TGSP) images (labeled 1'-5'). The line intensity ratio Al1/4C for each TGSP shown with diamonds changes from the minimum value of 0.3 (1st frame) to the maximum value of 1 (4th frame).

FIG.2. TGSI spectra. Modeling of L-shell Cu radiation from shot 1293 (DPWA) shows that Te is gradually increasing during the development of the x-ray burst up to 300 eV

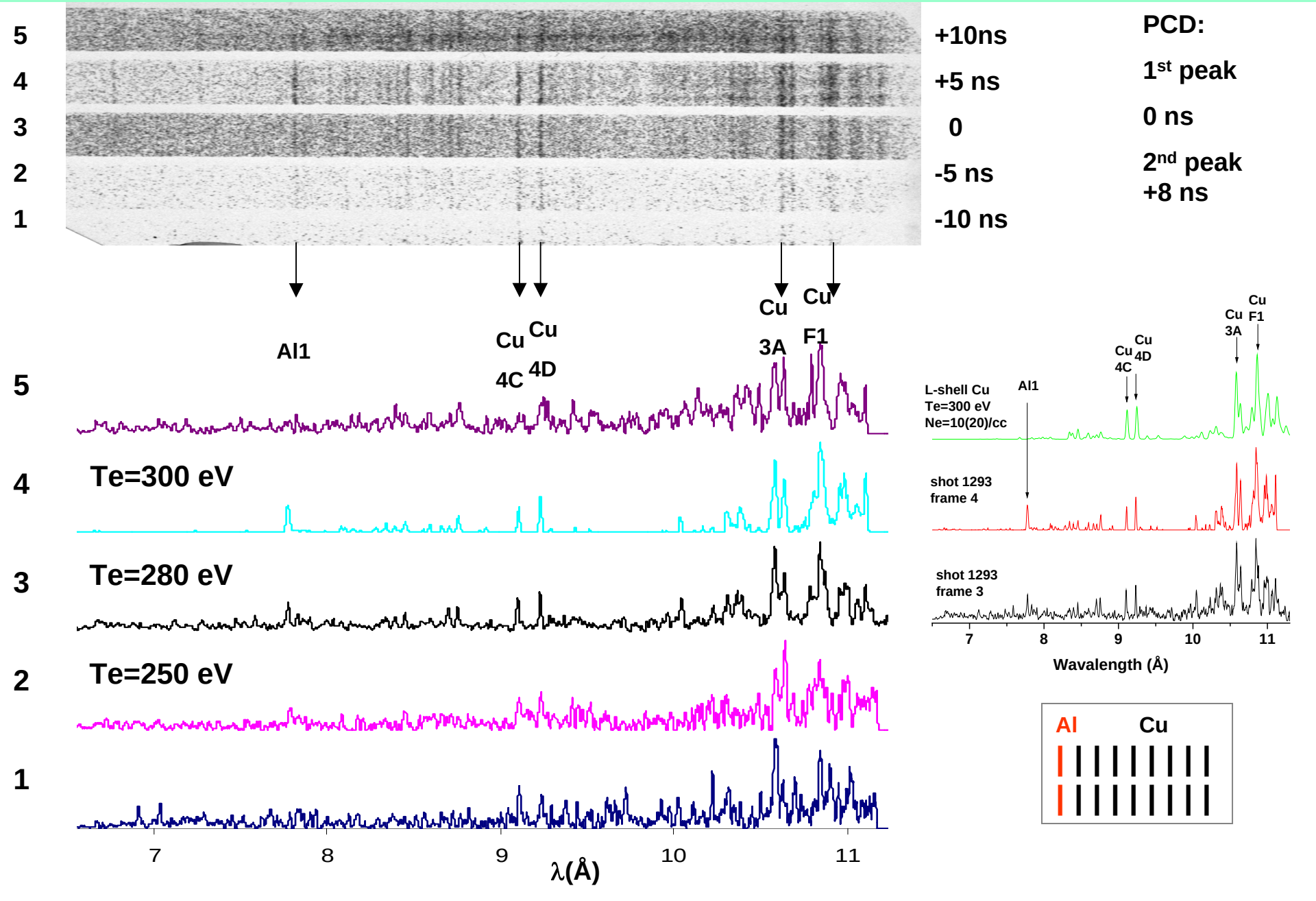

X-ray time-gated pinhole images and spectra and their analysis (continued)

According to the simulations with the wire ablation dynamics model (WADM) [4] the outermost wires of the planar array ablate and implode first. Thus we can expect that a significant mass fraction of the Al wires, which were positioned initially at the array periphery, should be ablated and transported to the array center during the first half of the current pulse. However, the x-ray image of TGSP (see the top of Fig. 2) indicates that the Al1 line barely seen in first two frames increases in intensity and reaches maximum during the time of 4^{th} frame (in comparison with L-shell Cu radiation). For example, the ratio of intensities Al1/4C plotted at the top of Fig. 1 changes from 0.3 (1^{st} frame) to 0.8 (3^{rd} frame and main x-ray burst) and to 1 (4^{th} frame). The electron temperature modeled from L-shell Cu spectra expresses similar behavior: it increases from 250 eV (2^{nd} frame) to 280 eV (3^{rd} frame and the main x-ray burst) to 300 eV (4^{th} frame). Theoretical spectrum calculated at Te=300 eV reproduces well the spectral features recorded by frame 4.

4. V.L. Kantsyrev, L.I. Rudakov, A.S. Safronova et al, Phys. Plasmas 15, 030704 (2008)

X-ray axially resolved time integrated spectra and their analysis

Time-integrated spatially resolved spectra (TISR) of implosions of SPWA and DPWA (recorded also by the KAP crystal) are presented in Fig. 3. First, the intensity of the most intense K-shell line Al changes very little from the anode to the cathode for SPWA than that for DPWA (in comparison with L-shell Cu lines). It might be explained by the more "column"-like plasma formation for SPWA (see Fig. 4) compared to "hot spot"- like plasma formation for DPWA (see Fig. 1). The WADM simulations, performed in Ref. [4], suggest that unlike the case of SPWA, where the precursor plasma column and the resultant Z-pinch are formed in the plane of the array wires, in the case of DPWA both the precursor column and Z-pinch are formed outside the wire planes, at the array center. Three-dimensional MHD simulations [10] suggests that for SPWA the proximity of the innermost array wires to the precursor column may enhance the stability of resultant Z-pinch, making it a "column"-like plasma object. This is clearly seen in Fig. 5 where the change of different line ratios with the distance from the anode is plotted. For example, the ratio Al1/4C is about 0.7 for SPWA and is almost constant from the anode to the cathode while for DPWA it changes from 0.35-0.55 near the anode to 0.8 in the middle and near the cathode.

4. V.L. Kantsyrev, L.I. Rudakov, A.S. Safronova *et al*, Phys. Plasmas 15, 030704 (2008)

10. A.A. Esaulov, V.L. Kantsyrev, A.S. Safronova *et al*, "Magnetostatic and magnetohydrodynamic modeling of planar wire arrays", Phys. Plasmas 14 (5), in print (2008).

Fig. 3. Axially resolved spectra from SPWA (Zebra shot 782, left) and DPWA (Zebra shot 1293, right). Diagnostically important lines are labeled with Al1-Al3 for K-shell Al and Cu 4C-Cu 6C for L-shell Cu spectra

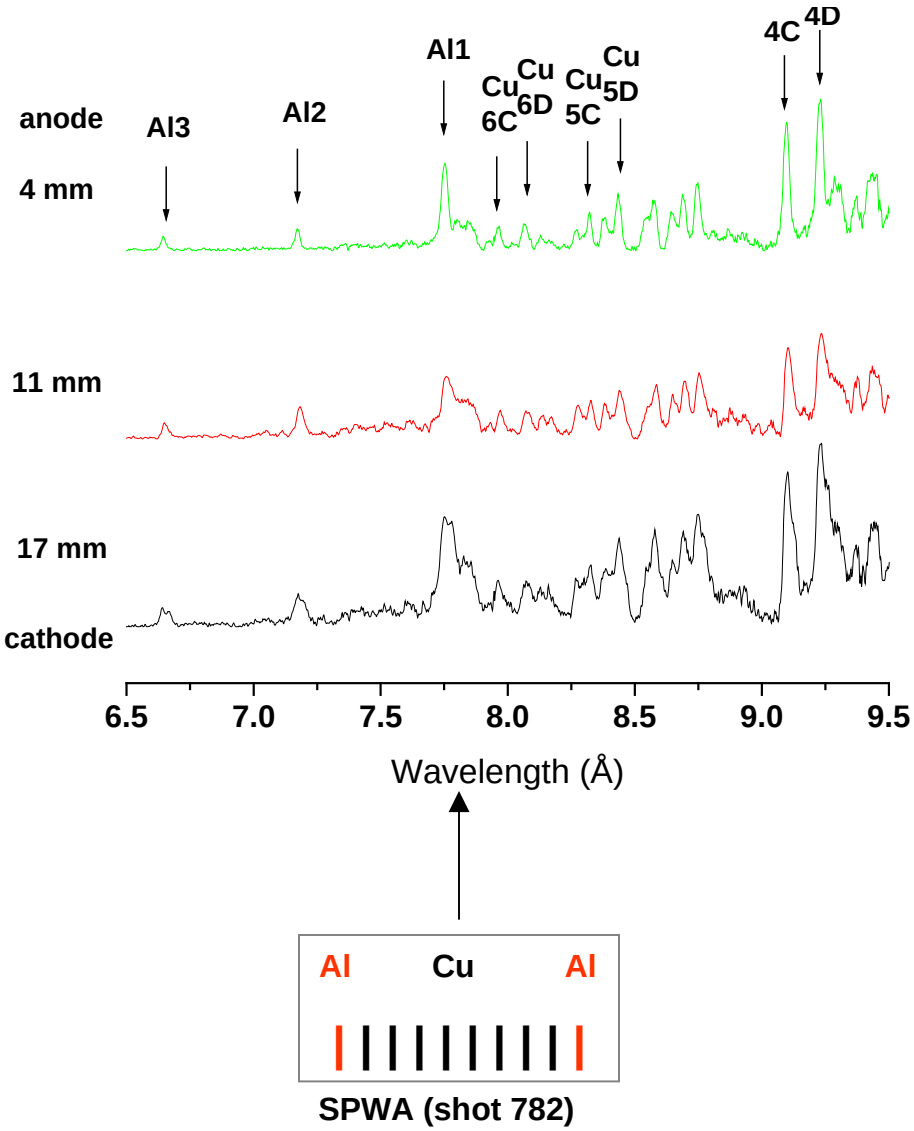

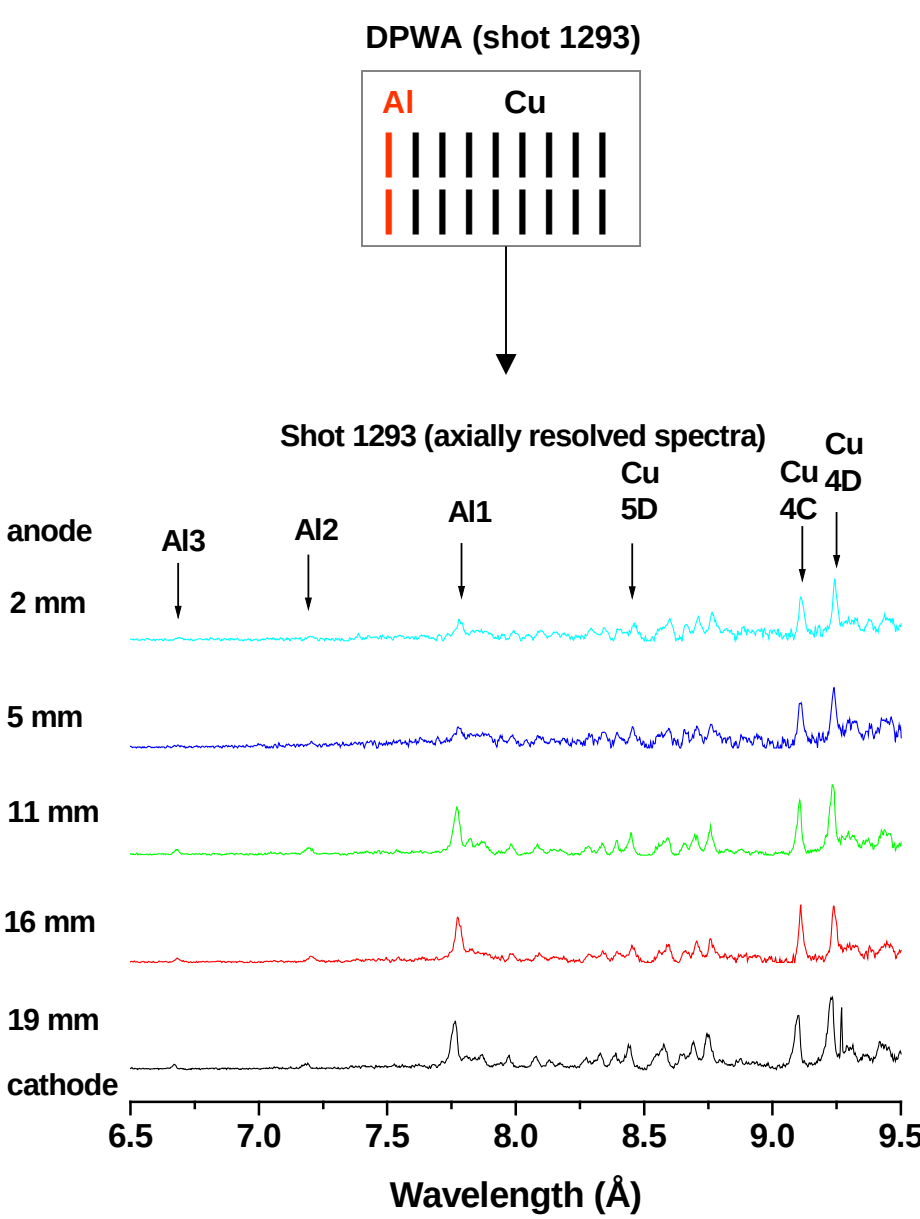

$(Al2/Al1)_{max}$=0.54 at 11 mm from the anode for shot 782

Fig. 4. Zebra shot 782. PCD (8 μm Be filter) detector that registered x-ray radiation with hν > 0.75 keV (gray) and current (red) data. Note more "column"- like plasma formation for SPWA

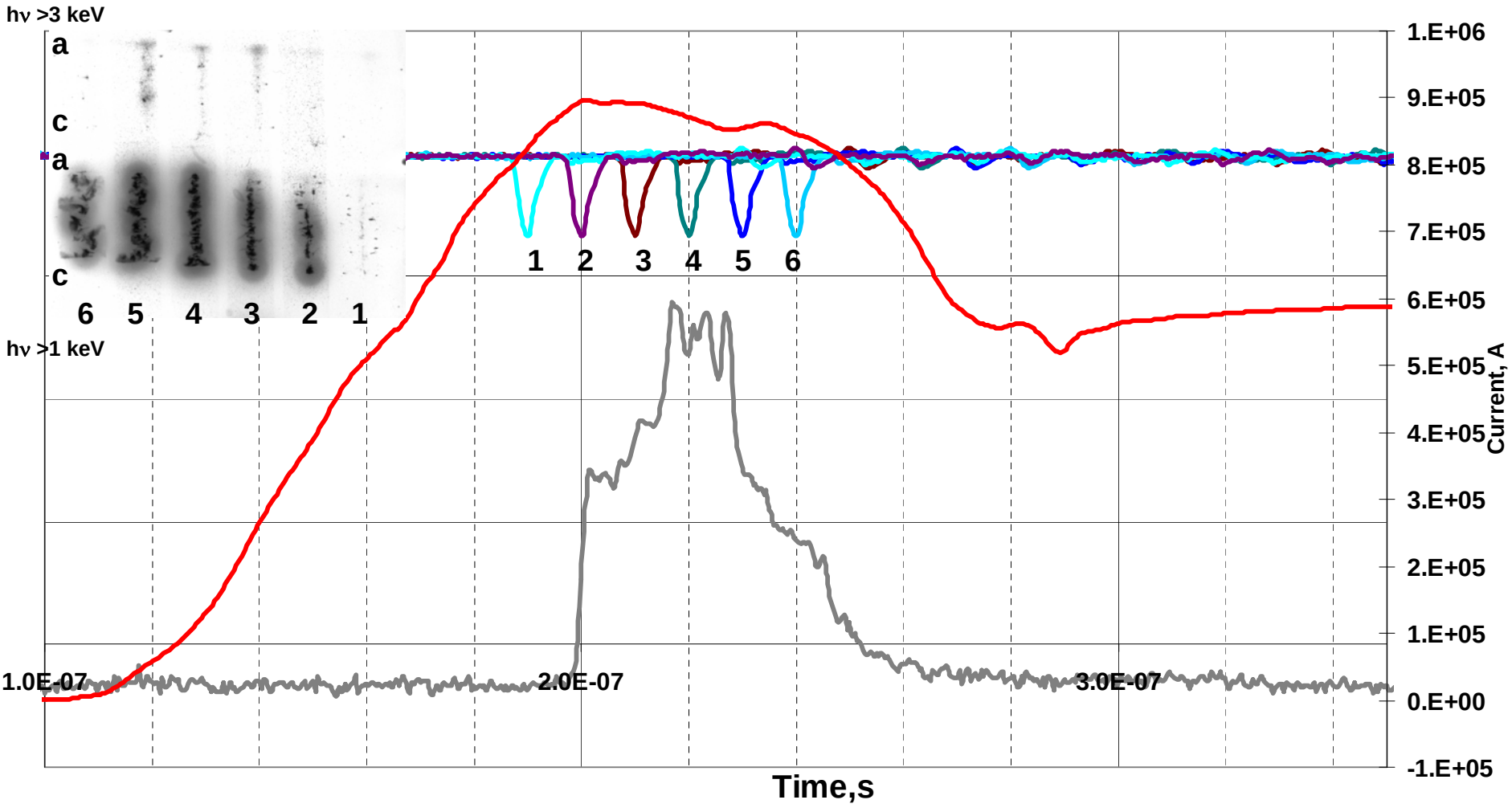

X-ray axially resolved time integrated spectra and their analysis (continued)

Second, the axial gradients in the temperature Te manifest more for DPWA than for SPWA due to the same reason. To illustrate it, ratios of intensities F1/3A and 4C/F1 are plotted in Fig. 5 which are sensitive to the temperature Te. For example, the ratio F1/3A (more sensitive to Te than 4C/F1) equal or greater than 1 at moderate densities indicates Te ≥ 280 eV and changes only slightly between 1.1 and 1.2 for SPWA and more between 0.8 and 1.1 for DPWA. Therefore, the ratios indicate that the temperature Te from L-shell Cu is larger near the cathode for both SPWA and DPWA. In addition, it is important to study the ratios of K-shell Al lines Al2/Al1 and Al3/Al1. For SPWA, both ratios reach the maximum values Al2/Al1=0.57 and Al3/Al1=0.29 in the middle (at 11 mm from the anode) which are almost double than near the cathode. Such big ratio of Al2/Al1 indicates the temperature Te of K-shell Al plasma at least 100 eV higher than that from L-shell Cu plasma (at 11 mm from the anode). Also for SPWA the broadening of K-shell Al lines changes with the distance and is maximum at 11 mm from the anode that might indicate the stronger influence of opacity effects in the middle (for L-shell Cu lines also) and almost no influence of it near the anode. Inclusion of opacity effects for K-shell Al will lower Te bringing it closer to Te from L-shell Cu (for the spectra in the middle). The opposite situation was found for DPWA: no opacity effect was observed for K-shell Al lines (see Fig. 3, on the right). The ratios Al2/Al1 and Al3/Al were very small (less than 0.15) and almost unchanged from the middle to the cathode and no substantial broadening was observed. This can be explained by the less concentration of Al in the total wire array mass (11.3 % for DPWA vs 18.5% for SPWA).

Fig. 5. Diagnostically important line ratios from axially resolved spectra shown in Fig. 3 for Zebra shots 782 and 1293

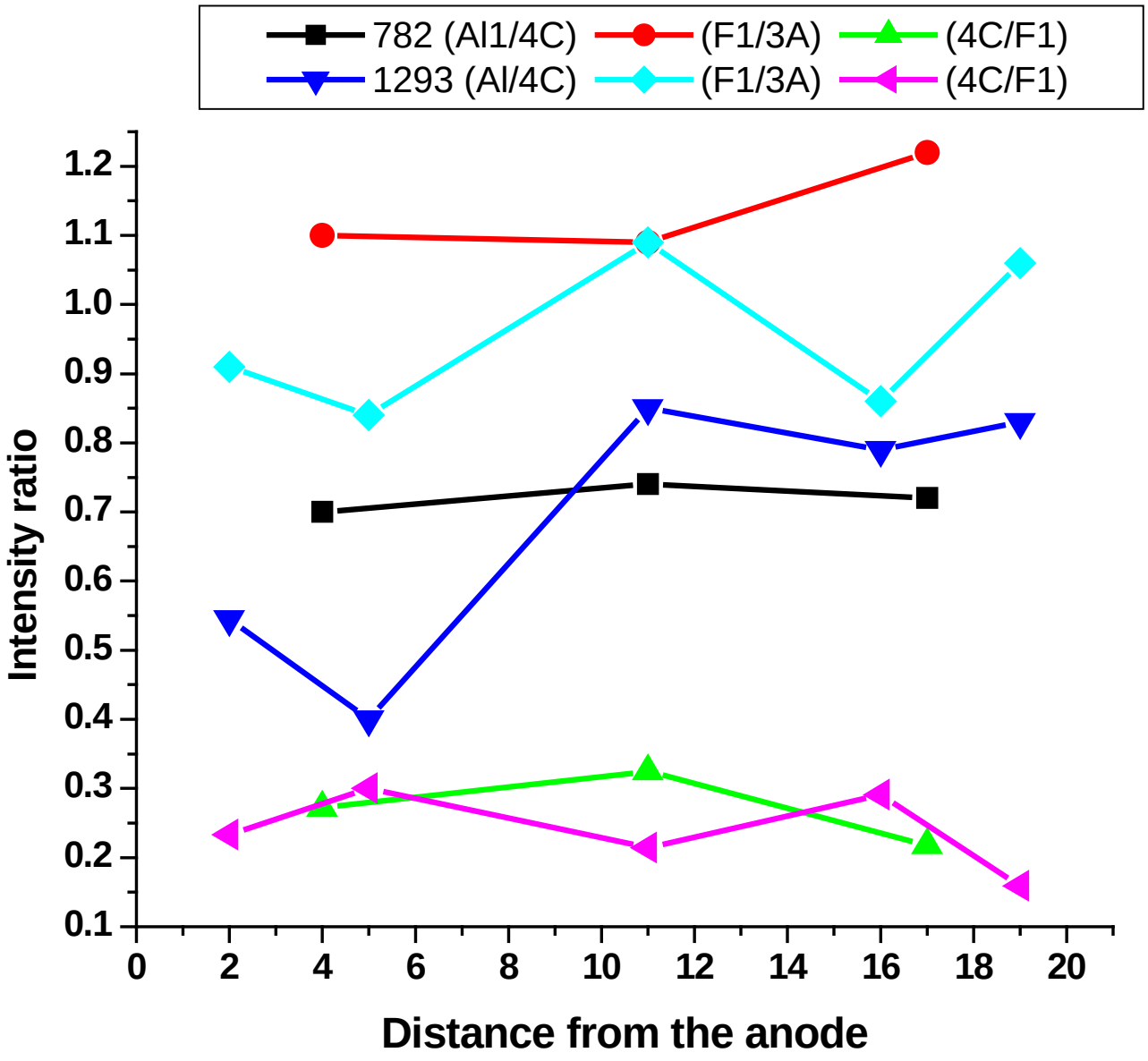

Fig. 5 (expanded set of data, more ratios). Diagnostically important line ratios from axially resolved spectra shown in Fig. 3 for Zebra shots 782 and 1293

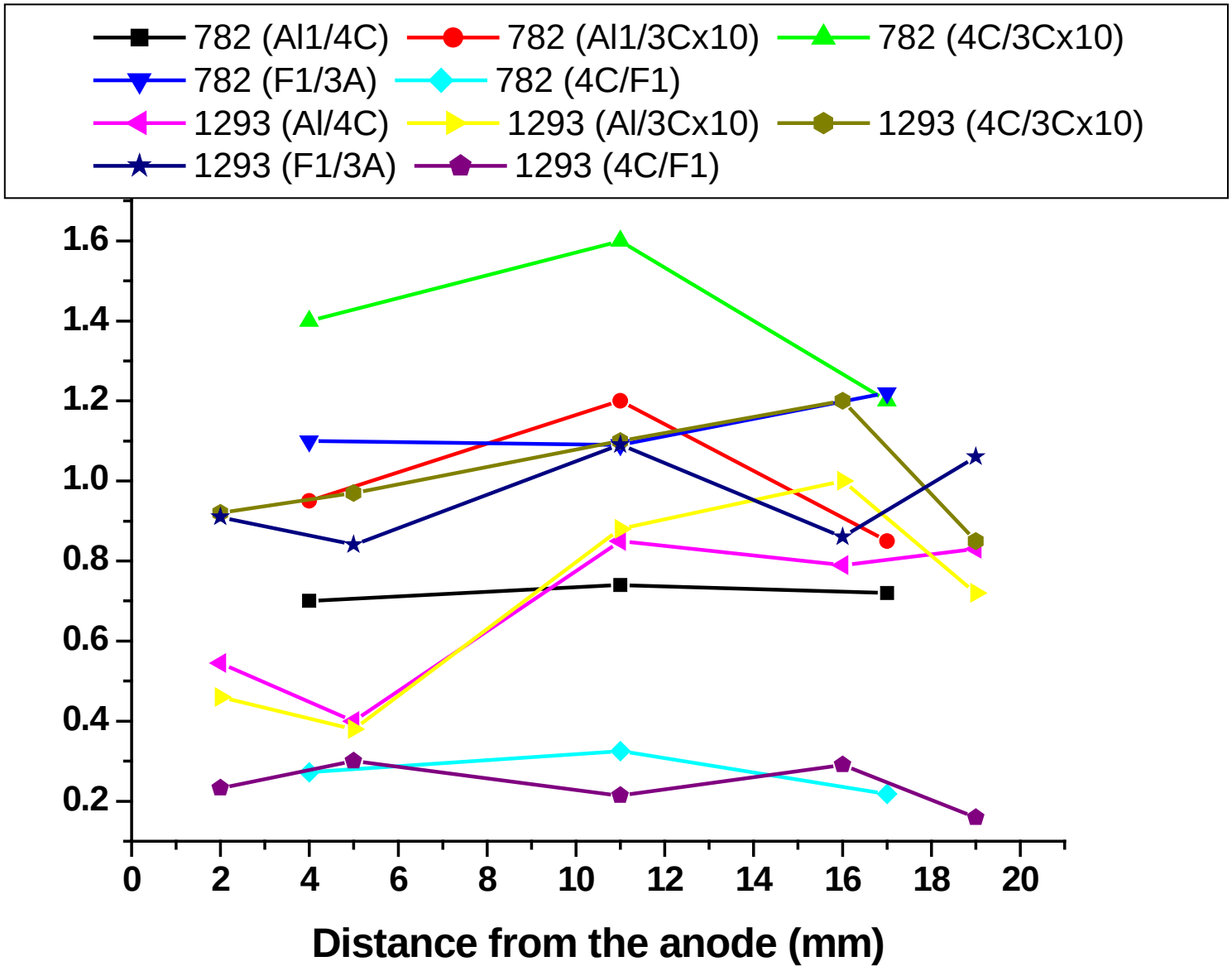

SPWA vs. DPWA implosion from WADM

SPWA

22 ns (-111 ns)

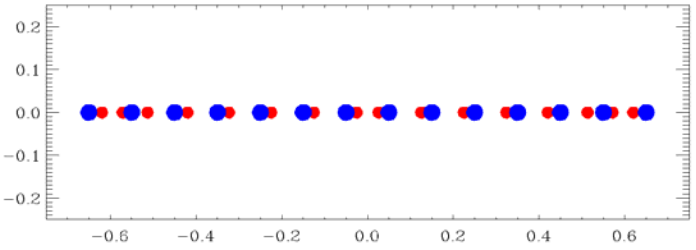

101 ns (-32 ns)

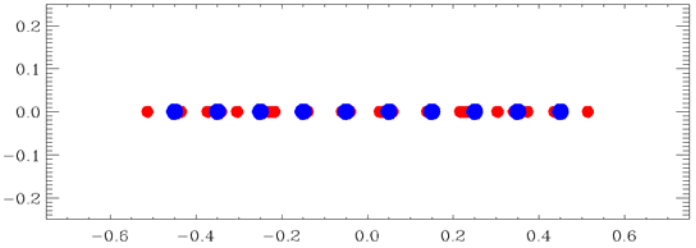

118 ns (-15 ns)

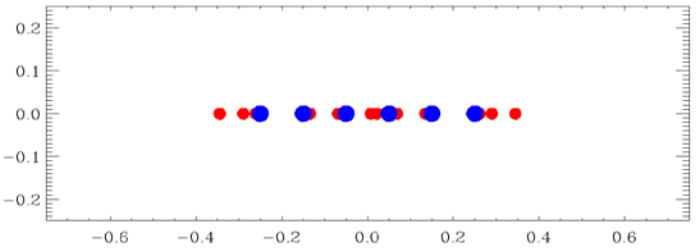

132 ns (-1 ns)

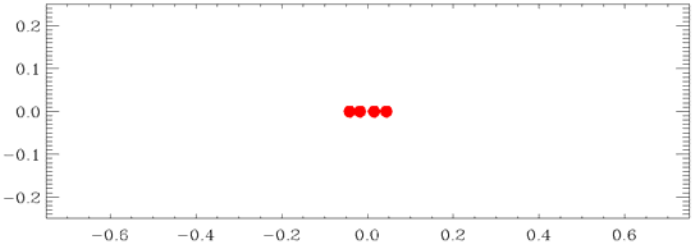

DPWA

13 ns (-80 ns)

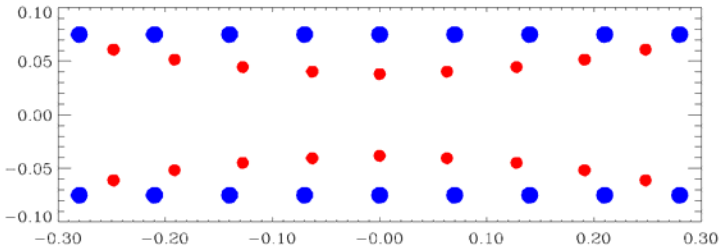

71 ns (-22 ns)

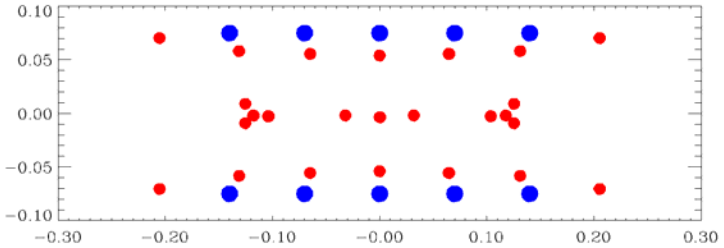

88 ns (-5 ns)

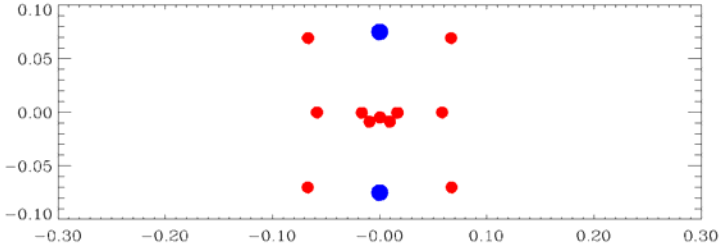

92 ns (-1 ns)

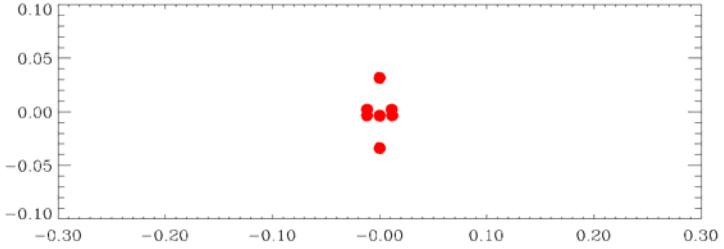

Axially resolved Al K-Shell spectra from the Al-5052 SPWA (Zebra Shot 801)

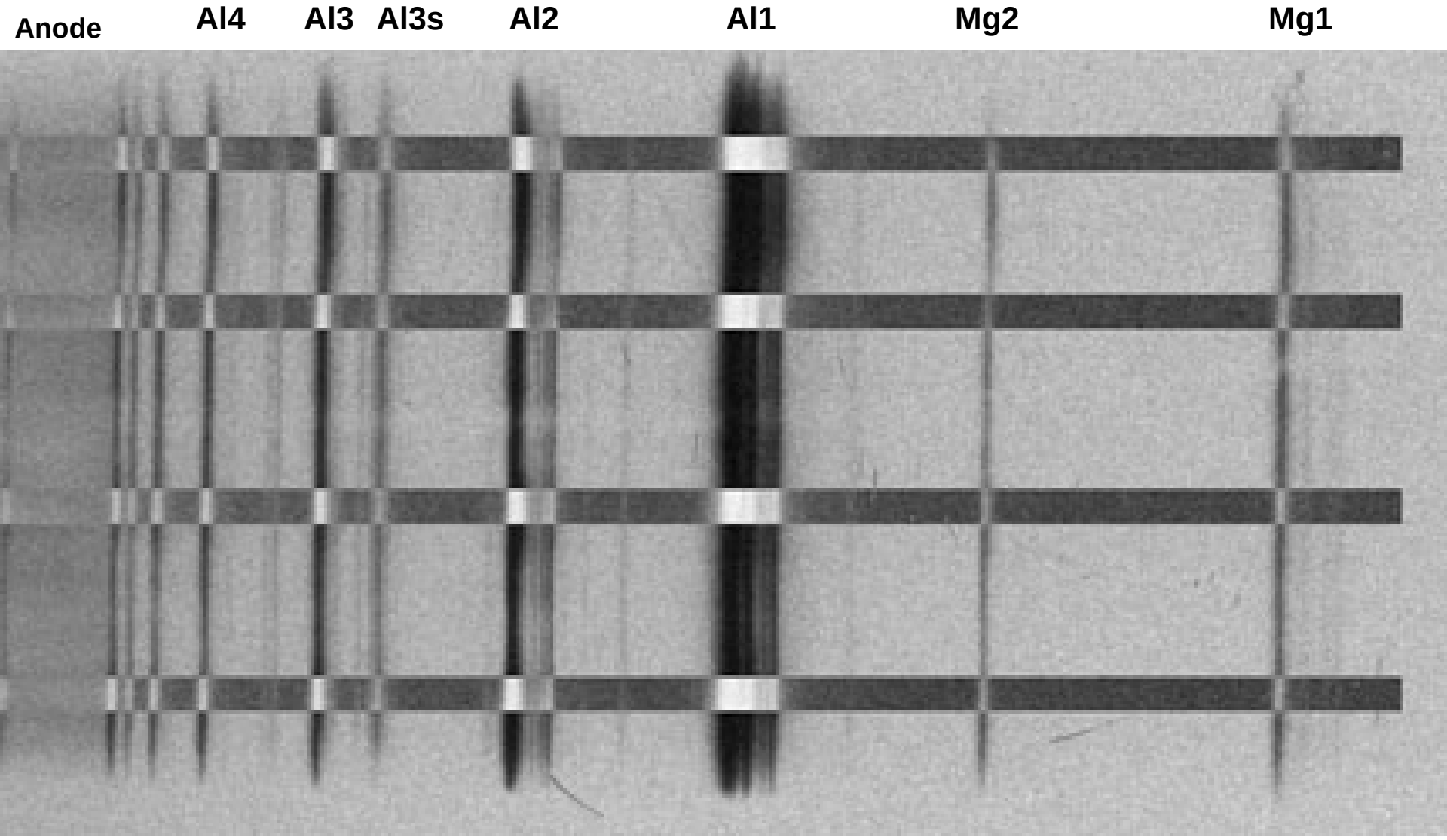

Modeling of axially resolved Al K-Shell spectra from the Al-5052 SPWA

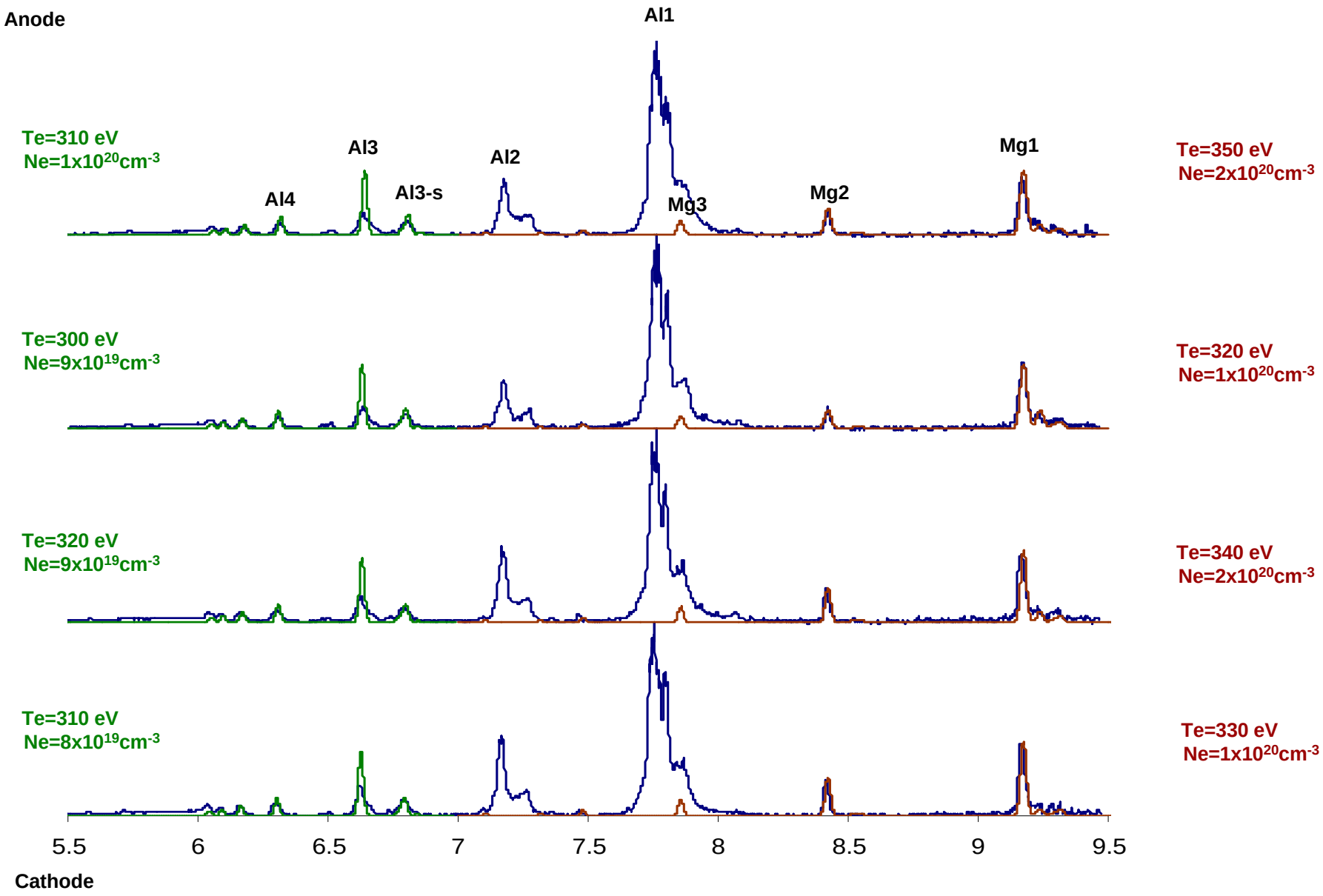

ACKNOWLEDGMENTS

This work was supported by NNSA under DOE Cooperative Agreements DE-FC52-06NA27588, DE-FC52-06NA27586, and in part by DE-FC52-06NA27616. Sandia is a multi-program laboratory operated by Sandia Corporation, a Lockheed Martin Company, for the United States department of Energy under Contract DE-AC04-94AL85000.